

**ARTICLE**

# Optimization of Transducer Location for Novel Non-Intrusive Methodologies of Diagnosis in Diesel Engines

S. Narayan<sup>1,\*</sup>, M. U. Kisan<sup>2</sup>, Shitu Abubakar<sup>2</sup>, Faisal O. Mahroogi<sup>3</sup> and Vipul Gupta<sup>4</sup>

<sup>1</sup>Department of Mechanical Engineering, Qassim University, Buraydah, 51452, Saudi Arabia

<sup>2</sup>Department of Mechanical Engineering, Ahmadu Bello University, Zaria, 810211, Nigeria

<sup>3</sup>Department of Mechanical Engineering, Islamic University of Madina, Medina, 42351, Saudi Arabia

<sup>4</sup>Department of Mechanical Engineering, Indus International University, Una, 174301, India

\*Corresponding Author: S. Narayan. Email: rarekv@gmail.com

Received: 18 March 2021 Accepted: 07 June 2021

**ABSTRACT**

The health monitoring has been studied to ensure integrity of design of engine structure by detection, quantification, and prediction of damages. Early detection of faults may allow the downtime of maintenance to be rescheduled, thus preventing sudden shutdown of machines. In cylinder pressure developed, vibrations and noise emissions data provide a rich source of information about condition of engines. Monitoring of vibrations and noise emissions are novel non-intrusive methodologies for which positioning of various transducers are important issue. The presented work shows applicability of these diagnosis methodologies adopted in case of diesel engines. The effects of changing various fuel injection parameters was analyzed. Scope of using non-intrusive technique has been analyzed by changing locations of microphone. Novelty of this work lies in exploring signal processing methods for various locations around the engine test set up. Various frequency ranges of contributing noise and vibration sources were identified. Time-Frequency analysis showed the onset of various cyclic. Based on the identification of various frequency bands, it is possible to device suitable filters in order to extract more information.

**KEYWORDS**

IC engines; automotive; vibrations and noise emissions; condition monitoring; specialized industrial machinery and equipment

**1 Introduction**

Various sources of noise and vibrations in an automotive systems are shown in Fig. 1 [1–18].

Combustion based noise can be analyzed by monitoring the speed of combustion. It is generated as an impulsive pressure wave [19]. Motion based noise which is proportional to operational speed of engine, includes noise due to piston motion, bearing noise, cam noise, oil pump noise, timing belt and chain noise as well as structural noise of cover [20,21]. Aerodynamic flow noise includes contributions due to intake noise, exhaust noise and noise due to motion of fan. Wind and road tire noise lie in the medium frequency ranges [22]. Tab. 1 presents comparisons of features of various sources of noise in engines.



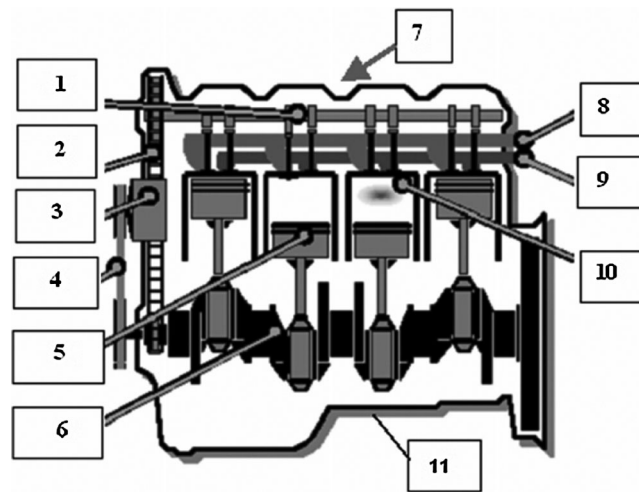


**Figure 1:** Sources of automotive noise (1: valve train motion, 2: chain drive motion, 3–4: accessory noise, 5: piston slapnoise, 6: bearing noise, 7: cover noise, 8: intake noise, 9: exhaust noise, 10: combustion noise, 11: oil pan noise)

**Table 1:** Characteristic features of various sources

Noise source	Approximate frequency range	Effecting factor
Combustion Noise	500–8000 Hz	In cylinder pressure
Piston Slap	2000–8000 Hz	Speed, piston design
Valve Operation	500–2000 Hz	Valve type, Engine speed
Fan Noise	200–2000 Hz	Speed, number of Blades
Intake Flow Noise	50–5000 Hz	Turbulence
Exhaust Flow Noise	50–5000 Hz	Turbulence
Injection Pump Operation	2000 Hz	Pump features
Gear Noise	4000 Hz	Speed, Number of teeth
Accessory Belt-Chain Noise	3000 Hz	Engine speed, misalignment, number of teeth

Among the advanced techniques, monitoring of noise and vibration emissions from engines, are important benchmarks for various choice of customers [11–21]. Various diagnosis methodologies adopted in case of diesel engines for their condition monitoring includes:

A. Monitoring of structural vibrations-optimumlocation of accelerometer transducer is a major hurdle as there may be contamination of signals. Frequency spectrum, peak or RMS values are effective to monitor various faults like imbalances, bearing damage or shaft misalignments [1].

B. Noise monitoring- injector operational faults, wear, incorrect injection timings, valve operation faults may be diagnosed by monitoring noise emissions from engine.

C. Cylinder pressure development monitoring-location of abnormal combustion and hence overall combustion efficiency of engines can be monitoring by profile of pressure developed inside combustion

chamber. However, higher operational temperatures conditions make various pressure sensors expensive with short life span time [2].

Attributes such as durability and serviceability requires a vehicle to be in service for certain period of time. Costs of vibration and noise control are usually very high, e.g., the yearly costs of warranty for brake was about 1 Billion U.S. \$. during the year 2005 [23–40]. So it is necessary to focus on NVH aspects of combustion engines.

## 2 Background

Various signal processing methods that may be used for effective condition monitoring of engines includes:

A. Power spectral density function (PSD)—This function ( $\Psi^2$ ) provides the frequency composition of data in terms of its mean square values [4]. The mean square values of a time sample in frequency range  $[\omega, \omega + \Delta\omega]$  can be obtained by passing sample through a band pass filter with sharp cut off frequency features and then computing the average of squared output from filter.

B. Time frequency analysis—This analysis is useful as long as frequency content of signals do not vary with time. Hence time frequency analysis or wavelet analysis are more suitable for analysis of transient signals [5]. In the time frequency analysis, the signal is windowed into small intervals and then Fourier transformation is taken for each interval [6–29]. Length of window can be used to change the resolution of the output signal. A shorter window has higher resolution in time domain, but a poor resolution in frequency domain and vice versa.

## 3 Literature Review

Dev Prakash Satsang investigated the efficacy of different diesel/n-butanol blends in a direct injection diesel genset engine [30]. Syed et al. recorded vibration signatures from an engine operated with ZnO particles suspended in Jatropha Methyl Ester (JME) biodiesel [31]. An artificial Neural Network (ANN) modelling was used to predict Root Mean Square (RMS) of velocity. Liu et al. [32]. developed random analysis procedure to predict the structural response of railway vehicle. Wang et al. [33] proposed a numerical method for NVH design sensitivity. Sofiyev et al. [34] analysed vibration of truncated conical shells made of functionally graded material. Jayaswal et al. [35] provided a review of ANN, fuzzy logic and wavelet transform in fault diagnosis in rolling bearings. Li et al. [36] achieved source separation using acoustic signals. Yildirim et al. [37] analysed noise and vibration of cars by feedforward and radial basis neural networks. Amezcua et al. [38] demonstrated accelerometer can provide sufficient combustion information. Morello et al. [39] analyzed crankshaft vibration to locate slapping motion of the skirt and combustion noise. In Jia et al. [40] concluded that the accelerometer signals were significantly influenced from a mechanical noise sources due to the start of injection. Research into the estimation of diesel engine combustion metrics via remote combustion sensing has become an increasingly active area of combustion research [41]. For reduction of engine-out emissions and improvement of fuel economy, closed-loop control of the combustion process has been explored and documented by many researchers [42]. A novel bi-directional non-negative matrix factorization (GBiNMF) algorithm was proposed to find a parts-based representation of the TFRs corresponding to different fault models [43,44]. An estimation method of the combustion chamber pressure, in an internal combustion engine was created based on the comparison of the vibration and pressure signals [45–59].

## 4 Material and Methods

Experiments were conducted on a KPKN2520 type kirloskar diesel rig having specifications as presented in Tab. 2. Various testing conditions are enlisted in Tab. 2. Testing case with fuel injected at 3600 RPM engine speed and 700 Bar injection pressure was taken as references.  $1 \text{ mm}^3/\text{stroke}$  of fuel

was injected during pre -injection period as well as main injection period at crank angle positions  $6^\circ$  and  $10^\circ$  before top dead center positions of for this case.

**Table 2:** Engine specification

Type	Single cylinder DI 4 stroke diesel engine
Cooling	Air cooled
Rated power	3 kW@1500 RPM
Bore X Stroke	80 mm $\times$ 110 mm
Compression ratio	17.5:1

An AVL GU13P type piezoelectric transducer was used to acquire the instantaneous in-cylinder pressure data having various features enlisted in [Tab. 3](#).

**Table 3:** Pressure transducer specifications

Range	0–200 Bar
Sensitivity	15.8 pC/Bar
Resonant frequency	130 kHz

Various block vibrations were recorded by Endveco7240C make Mono axial accelerometers having features shown in [Tab. 4](#).

**Table 4:** Accelerometer transducer specifications

Range	0–1000 g
Sensitivity	15.8 pC/Bar
Resonant frequency	90 kHz

A 4939 type Bruel and Kjaerfree-field  $\frac{1}{4}$ " make microphone having a preamplifier (type 2670) was used to acquire various noise emission signals. Main features of this transducer are shown in [Tab. 5](#).

**Table 5:** Microphone transducer specifications

Range	28–164 dB
Sensitivity	4 mV/Pa
Resonant frequency	4–100 kHz

## 5 Results and Discussions

In order to analyze noise emissions at various locations, a grid was built around the test engine to change the location of microphone. Particular attention was focused on three positions marked A, B, C as depicted in [Fig. 2](#). [Figs. 3](#) and [4](#) show recorded noise emissions at three chosen locations under full 100% load conditions

and speed of 1600 RPM and 2000 RPM. It can be observed that all traces have low frequency oscillations related to firing frequency of engine. Position C is characterized by high frequency oscillations around 360° crank angle position due to onset of combustion events.

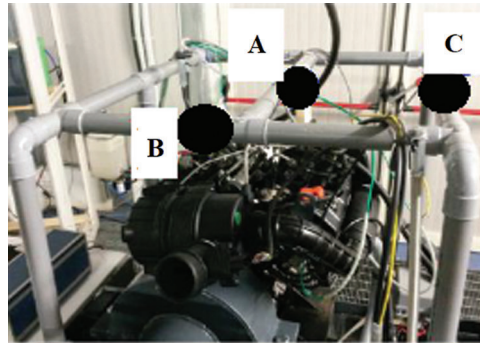


**Figure 2:** Three positions to acquire noise emissions

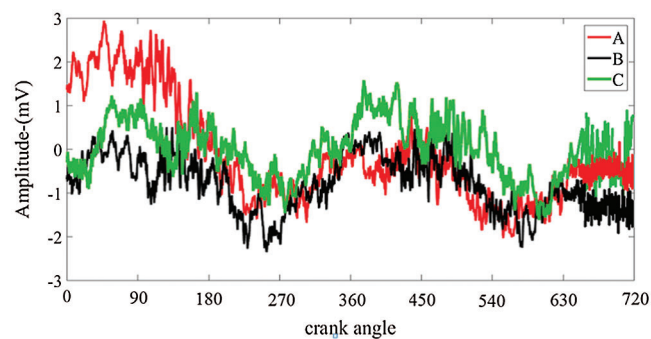


**Figure 3:** Noise emissions at 1600 RPM, 100% load

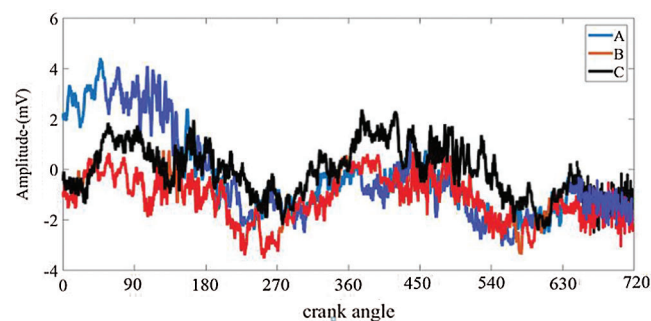


**Figure 4:** Noise emissions at 2000 RPM, 100% load

Position B was next investigated to see if any information could be extracted regarding intake flow noise. Figs. 5 and 6 show plot of intake pressures acquired at this position at various testing conditions. Absence of any noticeable changes in signals acquired shows that acoustic signals were least affected by load values.

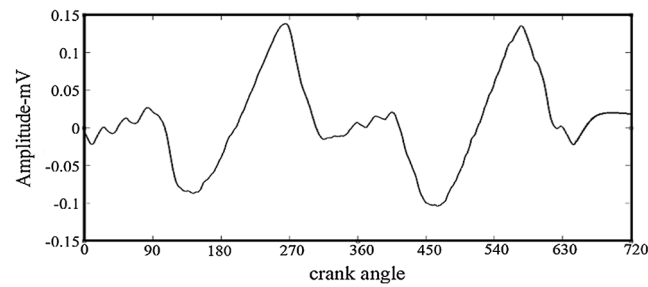


**Figure 5:** Intake pressure at 1600 RPM, 80% load

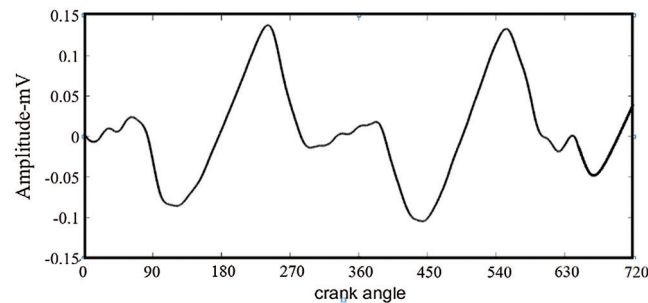


**Figure 6:** Intake pressure at 1600 RPM, 100% load

Further coherence function was used for analysis of signals. This function which is denoted as a normalized function that may be defined as the ratio between the square of cross power spectral densities of input and output signals to the product of the power spectral density (PSD) of individual signals. Figs. 7 and 8 show plot of coherence functions between intake pressure and noise radiated from engine at location B were computed using a Hanning window of length 1/6th of engine cycle. It may be observed that a close relationship exists between the two signals in frequency range [50 Hz–400 Hz] irrespective of load values. Such a band in which intake pressure signals are closely correlated with noise emissions is dependent on engine speed. In this frequency band, gas exchange process may be considered as a major contributor towards overall noise emissions.

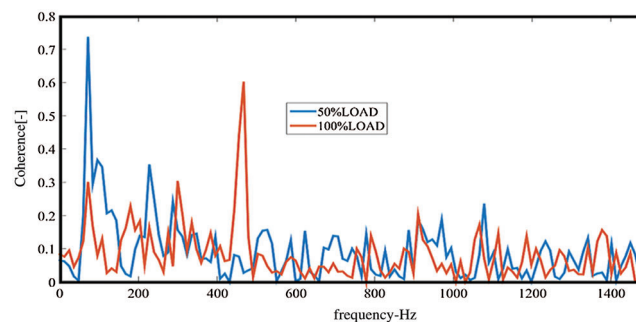


**Figure 7:** Coherence between cylinder pressure and intake pressure signals (100% load, 1600 RPM)

The noise emissions at location C were filtered in the above mentioned frequency range and compared with those of unfiltered noise emissions at location B as shown in Figs. 9 and 10. A close correlation between two signals shows the selected frequency band was properly chosen.

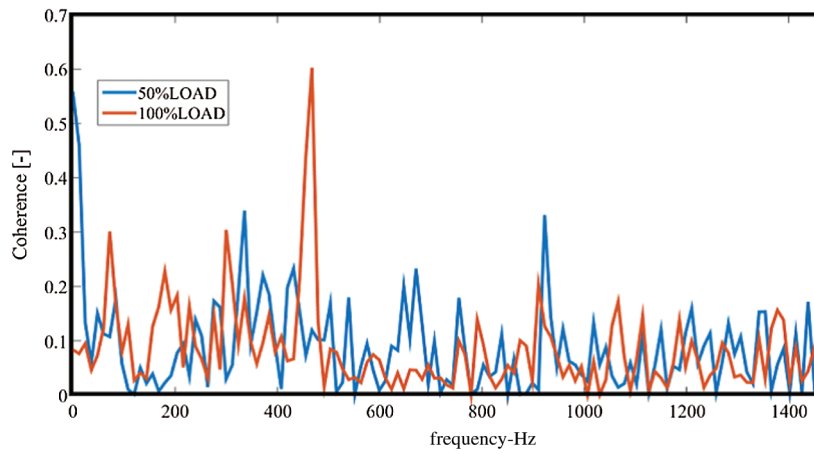


**Figure 8:** Coherence between cylinder pressure and intake pressure signals (100% load, 2000 RPM)

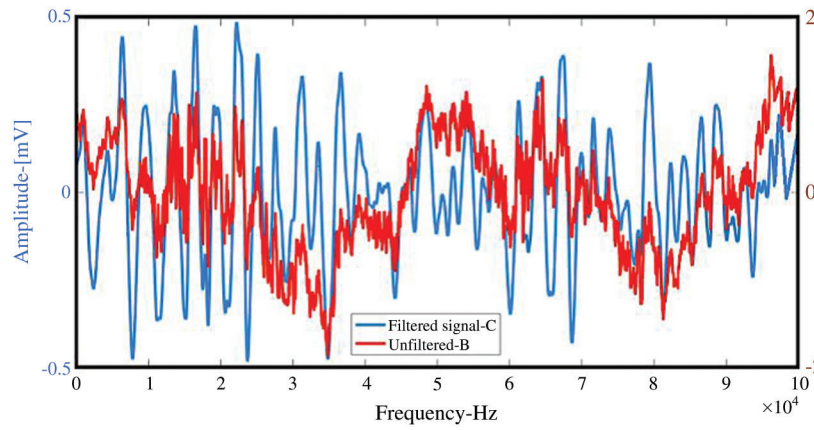


**Figure 9:** Comparison between signals (1600 RPM—100% load)

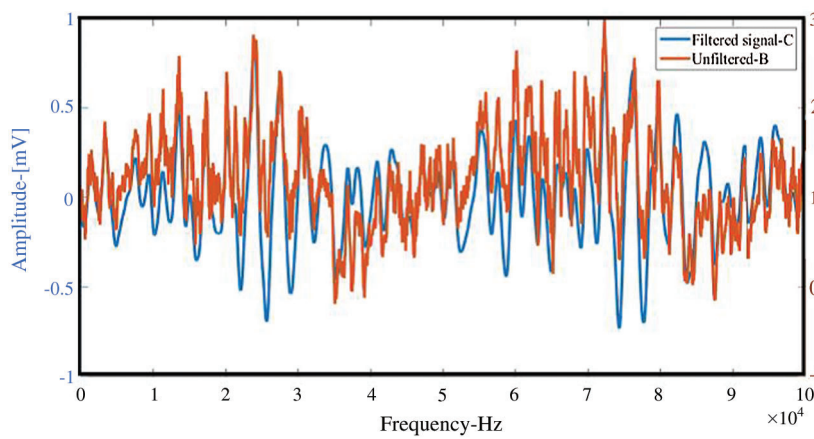


**Figure 10:** Comparison between signals (2000 RPM—100% load)

Further tests were done in order to investigate signals at various marked locations. PSD plots of various signals were analyzed using Pwelch function. Peaks were found in PSD plots of in cylinder pressure at frequencies which were integral multiples of fundamental firing frequency of engine. These plots highlight that main changes due to firing of fuel inside cylinder occurs at 300 Hz frequency (Figs. 11 and 12). Hence all combustion related events must be considered above this frequency.

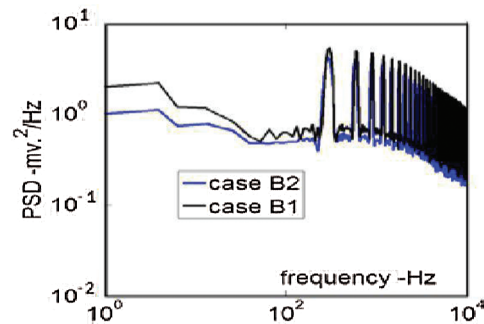


**Figure 11:** PSD plots for cylinder pressure signals (100% load, 1600 RPM)

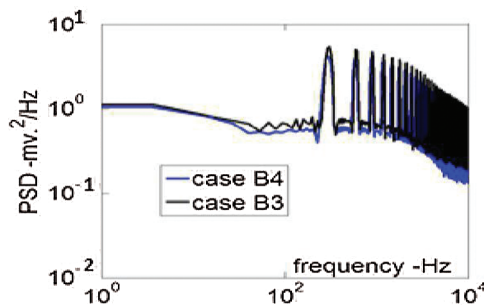


**Figure 12:** PSD plots for cylinder pressure signals (100% load, 2000 RPM)

Since the acoustic power radiated from engine also depends upon the block velocity, the velocity of in cylinder pressure evolution also represents an important term in study of combustion source. PSD plots of this parameter for given testing conditions were plotted as seen from Figs. 13 and 14. It is clear that the region 2 corresponding to medium frequency ranges of combustion noise begins after 1 kHz.

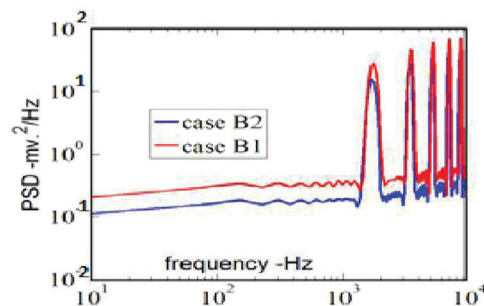


**Figure 13:** PSD plots for cylinder pressure derivative signals (100% load, 1600 RPM)



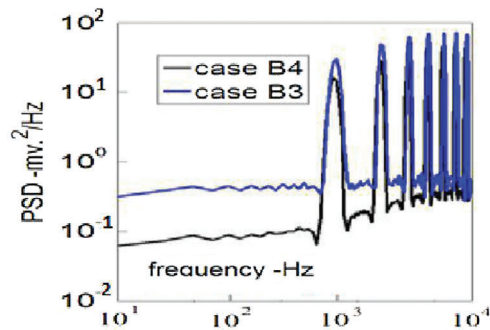


**Figure 14:** PSD plots for cylinder pressure derivative signals (100% load, 2000 RPM)

Further in cylinder pressure signals acquired at location C were studied using time-frequency spectrogram analysis as seen from Figs. 15–18. The frequency contents of signals were calculated by means of discrete Fourier transformation that were computed using FFT of overlapped windowed segments of signals. The color bars in these figures denotes the amplitude of components. Dark colors denote higher energy bands, whereas the lighter ones displays lower energy bands. High frequency components were found in frequency range 500 Hz–40 kHz owing to rapid increase in cylinder pressure after pre- injection period a few degrees before TDC position. Figs. 19 and 20 show the PSD plots for noise signals acquired both at motored as well as fired conditions using microphone located at position marked as A. It can be seen that contributions of combustion process towards noise emissions occurs at wider frequency bands when compared with cylinder pressure PSD plots. This may be due to several non-linear paths of noise propagation through engine as discussed in [7–17]. Noise PSD plots were characterized by high frequency components that may be due to several other contributing sources.

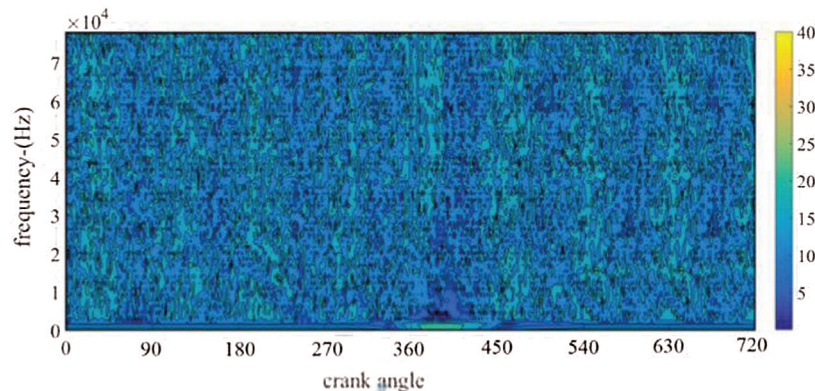


**Figure 15:** Cylinder pressure spectrogram at 1600 RPM, 100% load

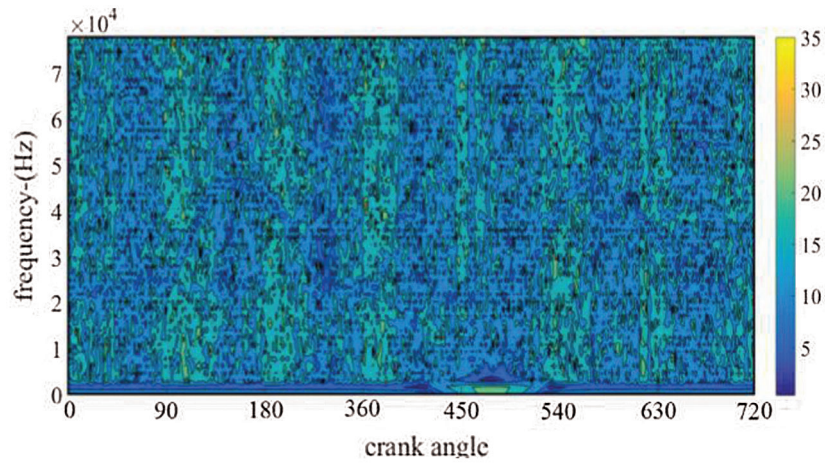


**Figure 16:** Cylinder pressure spectrogram at 1600 RPM, motored

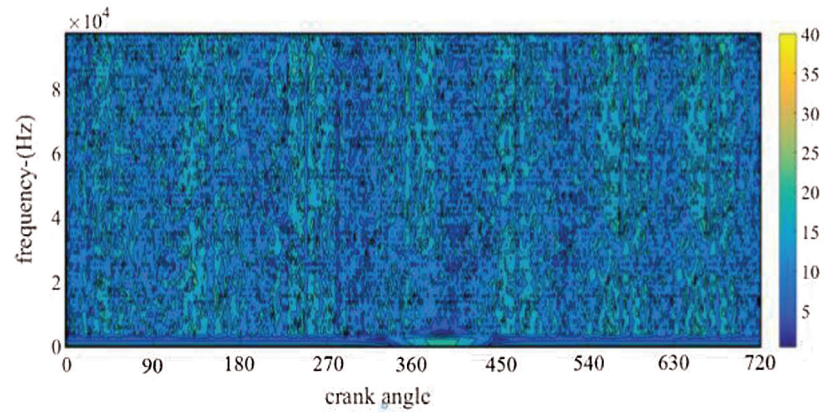


**Figure 17:** Cylinder pressure spectrogram at 2000 RPM, 100% load

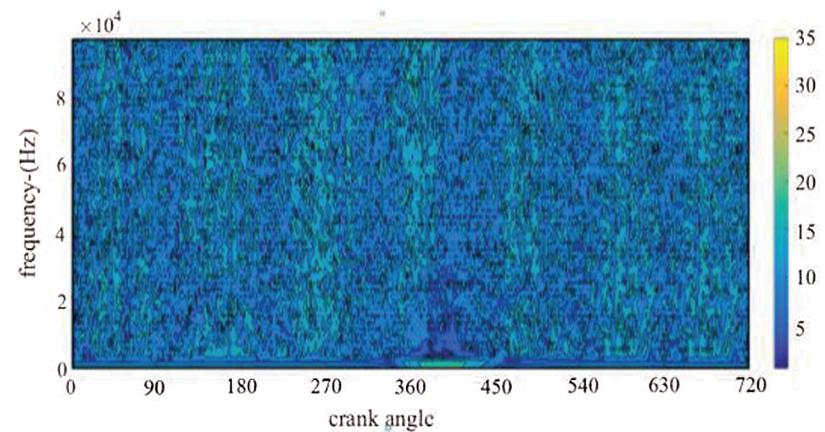


**Figure 18:** Cylinder pressure spectrogram at 2000 RPM, motored

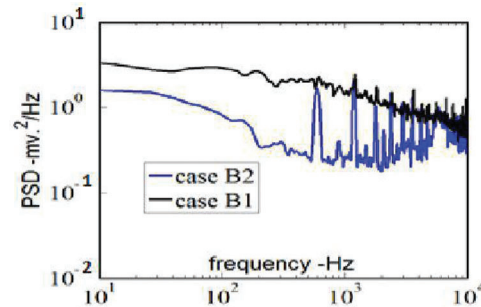


**Figure 19:** PSD plots for noise signals (100% load, 1600 RPM)

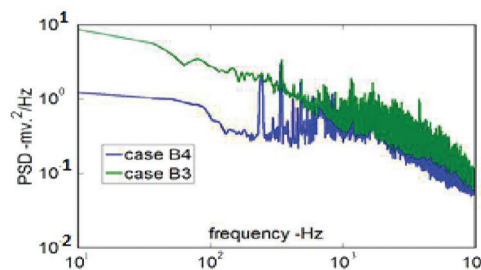


**Figure 20:** PSD plots for noise signals (100% load, 2000 RPM)

## 6 Conclusions

This work analysed the effects of change in various injection parameters on development of combustion pressure development and noise emissions from engines. Scope of using non-intrusive diagnosis technique has been analysed by using changing various locations of microphone around the engine. This work analysed the effects of changes in various injection parameters on development of combustion pressure and noise emissions from engines. Scope of using non-intrusive diagnosis technique has been analysed by changing various locations of microphone around the test engine. For this purpose, three positions were chosen denoted by A, B and C. Position C was seen as being most sensitive towards combustion process, position B was found to be sensitive towards intake process and finally position A was seen to have contribution of all other sources towards noise emissions. In particular, the noise emissions from engines were found to be dependent on quantity of fuel injected inside cylinder. Various characteristic frequency ranges of contributing sources have been identified. Time–Frequency analysis has shown onset of various events associated with working of engine. Based on the identification of various frequency bands, it is possible to device suitable filters in order to extract more information about combustion and motionbased noise which is done in later part of this work.

**Funding Statement:** The authors received no specific funding for this study.

**Conflicts of Interest:** The authors declare that they have no conflicts of interest to report regarding the present study.

## References

1. Saiteja, P., Ashok, B. (2021). A critical insight review on homogeneous charge compression ignition engine characteristics powered by biofuels. *Fuel*, 285, 119202.
2. Jacob, A., Ashok, B. (2020). An interdisciplinary review on calibration strategies of engine management system for diverse alternative fuels in IC engine applications. *Fuel*, 278, 118236.

3. Ashok, B., Nanthagopal, K., Chyuan, O. H., Karthickeyan, V., Tamilvanan, A. (2020). Multi-functional fuel additive as a combustion catalyst for diesel and biodiesel in CI engine characteristics. *Fuel*, 278, 118250.
4. Ashok, B., Jeevanantham, A. K., Bhat Hire, K. R., Kashyap, V., Saiteja, P. (2020). Calibration of idling characteristics for lemon peel oil using central composite design in light commercial vehicle diesel engine. *Energy Conversion and Management*, 221, 113183.
5. Ashok, B., Jeevanantham, A. K., Prabhu, K., Nadgauda, N. S., Karthick, C. (2021). Multi-objective optimization on vibration and noise characteristics of light duty biofuel powered engine at idling condition using response surface methodology. *Journal of Energy Resources Technology*, 143(4), 042301.
6. Kumar, A. N., Kishore, P. S., Raju, K. B., Nanthagopal, K., Tamilvanan, A. (2020). Decanol proportional effect prediction model as additive in palm biodiesel using ANN and RSM technique for diesel engine. *Energy*, 213, 119072.
7. Narayanasamy, B., Jeyakumar, N., Balasubramanian, D. (2021). Effect of star anise as a natural antioxidant additive on the oxidation stability of lemon grass oil. *Waste and Biomass Valorization*, 12, 2983–2997.
8. Ramalingam, K., Kandasamy, A., Balasubramanian, D. (2020). Forecasting of an ANN model for predicting behaviour of diesel engine energised by a combination of two low viscous biofuels. *Environmental Science Pollution Research*, 27, 24702–24722. DOI 10.1007/s11356-019-06222-7.
9. Karthickeyan, V., Ashok, B., Thiyagarajan, S. (2020). Comparative analysis on the influence of antioxidants role with *Pistacia khinjuk* oil biodiesel to reduce emission in diesel engine. *Heat and Mass Transfer*, 56, 1275–1292. DOI 10.1007/s00231-019-02797-6.
10. Vigneswaran, R., Balasubramanian, D., SabariSastha, B. D. (2021). Performance, emission and combustion characteristics of unmodified diesel engine with titanium dioxide (TiO<sub>2</sub>) nano particle along with water-in-diesel emulsion fuel. *Fuel*, 285, 119115.
11. EL-Seesy, I. A., He, Z., Hassan, H., Balasubramanian, D. (2020). Improvement of combustion and emission characteristics of a diesel engine working with diesel/jojoba oil blends and butanol additive. *Fuel*, 279, 118433.
12. Kaisan, M. U., Yusuf, L. O., Ibrahim, I. U., Abubakar, S., Narayan, S. (2020). Effects of propanol and camphor blends on emissions and performance of a spark ignition engine. *American Chemical Society Omega*, 5(41), 26454–26462.
13. Grujic, I., Stojanovic, N., Pesic, R., Davinic, A., Narayan, S. (2020). High-pressure hydrogen injection numerical analysis of IC engine operation with high pressure hydrogen injections. *Transactions of FAMENA*, 44, 55–56.
14. Mahroogi Faisal, O., Narayan, S. (2019). A recent review of hybrid automotive systems in GCC region. *Proceedings of Institute of Mechanical Engineers Part D: Journal of Automotive Engineering*, 234(7), 1393–1402.
15. Abubakar, S., Anafi, F., Kaisan, M., Narayan, S., Umar, S. (2020). Comparative analyses of experimental and simulated performance of a mixed-mode solar dryer. *Proceedings of the Institution of Mechanical Engineers, Part C: Journal of Mechanical Engineering Science*, 234, 1393–1402.
16. Kaisan, M. U., Abubakar, S., Ashok, B., Balasubramanian, D., Narayan, S. et al. (2021). Comparative analyses of biodiesel produced from jatropha and neem seed oil using a gas chromatography–mass spectroscopy technique. *Biofuels*, 12(7), 757–768. DOI 10.1080/17597269.2018.1537206.
17. Narayan, S., Gupta, V. (2018). Numerical analysis of secondary motion of piston skirt in engines. *International Journal of Acoustics and Vibrations*, 23, 557–565.
18. Narayan, S. (2014). A review of diesel engine acoustics. *FME Transactions*, 42, 150–154. DOI 10.5937/fmet1402150N.
19. Narayan, S., Milojevic, S., Gupta, V. (2019). Combustion monitoring in engines using accelerometer signals. *Journal of Vibro-Engineering*, 21, 1552–1563.
20. Mahroogi Faisal, O., Narayan, S., Gupta, V. (2018). Acoustic transfer function in gasoline engines. *International Journal of Vehicle Noise and Vibration*, 13(3), 270–280.
21. Narayan, S. (2013). Wavelet analysis of diesel engine noise. *Journal of Engineering and Applied Sciences*, 8, 255–259.
22. Narayan, S. (2015). Analysis of piston slap motion. *International Journal of Applied Mechanics and Engineering*, 20(2), 445–450.

23. Narayan, S. (2013). Piston slap noise in engines. *International Journal of Applied Engineering Research*, 8(14), 1695–1700.
24. Narayan, S. (2013). Effect of dwell time on noise radiated from diesel engine. *International Journal of Applied Engineering Research*, 8, 1339–1347.
25. Mustapha, M., Kaisan, M. U., Shitu, A., Narayan, S. (2018). Determination of wear metals debris concentration in aircraft engines. *International Journal of Innovative Technology and Exploring and engineering*, 8(11), 1339–1347.
26. Alsagri, A. S., Gupta, V., Narayan, S. (2018). Design and analysis of hybrid automotive suspension system. *International Journal of Mechanical and Production Engineering Research and Development*, 8(2), 637–642.
27. Alsagri, A. S., Mahroogi, F. O., Narayan, S. (2018). Design and analysis of double wishbone suspension systems for automotive applications. *International Journal of Mechanical and Production Engineering Research and Development*, 8, 1433–1442.
28. Stojanovic, N., Glisovic, J., Grujic, I., Narayan, S. (2020). Influence of size of ventilated brake disc ribs on air flow velocity. *International Journal of Advanced Science and Technology*, 29(1), 637–647.
29. Mahroogi, F. O., Narayan, S. (2020). Effects of dampers on piston slapping motion. *International Journal of Vehicle Noise and Vibration*, 16(1–2), 46–57.
30. Satsang, D. P., Tiwari, N. (2018). Experimental investigation on combustion, noise, vibrations, performance and emissions characteristics of diesel/n-butanol blends driven genset engine. *Fuel*, 221, 44–60.
31. Javed, S., Satyanarayana Murthy, Y. V. V., Baig, R. U., Nagarjuna Rao, T. (2016). Vibration analysis of a diesel engine using biodiesel fuel blended with nano particles by dual fueling of hydrogen. *Journal of Natural Gas Science and Engineering*, 33, 217–230.
32. Liu, I., Zhang, Y., Guo, H., He, W., Xie, S. et al. (2020). Random vibration analysis procedure of railway vehicle, vehicle system dynamics. *International Journal of Vehicle Mechanics and Mobility*, 58, 12.
33. Wang, S. (1999). Design sensitivity analysis of noise, vibration, and harshness of vehicle body structure. *Mechanics of Structures and Machines*, 27, 317–335.
34. Sofiyev, H., Schnack, E. (2012). The vibration analysis of FGM truncated conical shells resting on two-parameter elastic foundations. *Mechanics of Advanced Materials and Structures*, 19, 241–249.
35. Jayaswal, P., Wadhvani, A. K. (2009). Application of artificial neural networks, fuzzy logic and wavelet transform in fault diagnosis via vibration signal analysis: A review. *Australian Journal of Mechanical Engineering*, 7, 157–171.
36. Lif, W., Gua, D., Balla, Y., leung, C., Phipps, E. (2001). A study of the noise from diesel engines using the independent component analysis. *Mechanical Systems and Signal Processing*, 15, 1165–1184.
37. Yildirim, Ş., Erkaya, S., Eski, I., Uzmay, I. (2009). Noise and vibration analysis of car engines using proposed neural network. *Journal of Vibration and Control*, 15, 133–156.
38. Amezcua, E., Maldonado, B., Rothamer, D., Kim, K. (2020). Accelerometer-based estimation of combustion features for engine feedback control of compression-ignition direct-injection engines. *SAE Technical Paper 2020-01-1147*.
39. Morello, A. J., Blough, J., Naber, J., Jia, L. (2011). Signal processing parameters for estimation of the diesel engine combustion signature. *SAE International Journal of Passenger Cars—Mechanical Systems*, 4, 1201–1215. DOI 10.4271/2011-01-1649.
40. Jia, L., Naber, J., Blough, J. (2016). Review of sensing methodologies for estimation of combustion metrics. *Journal of Combustion*, 3, 1–9. DOI 10.1155/2016/8593523.
41. Wang, X., Cai, Y., Li, A., Zhang, W., Yue, Y. et al. (2021). Intelligent fault diagnosis of diesel engine via adaptive VMD-Rihaczek distribution and graph regularized bi-directional NMF. *Measurement*, 172, 108823.
42. Wang, Q., Sun, T., Lyu, Z., Gao, D. (2019). A virtual in-cylinder pressure sensor based on EKF and frequency-amplitude-modulation Fourier-series method. *Sensors*, 19, 3122. DOI 10.3390/s19143122.
43. Grajales, J. A., Quintero, H. F., Romero, C. A., Henao, E., López, J. F. et al. (2016). Combustion pressure estimation method of a spark ignited combustion engine based on vibration signal processing. *Journal of Vibroengineering*, 18, 4237–4247.

44. Lee, Y., Lee, S., Choi, H. (2019). Analysis of vibration on an engine block caused by combustion in a diesel engine. *International Journal of Automotive Technology*, 20, 187–195.
45. Andersson, I., McKelvey, T., Larsson, M. (2014). Detection of combustion properties in a diesel engine using block mounted accelerometers. *IFAC Proceedings*, 47, 11866–11871.
46. Kaisan, M. U., Nafiu, T., Habib, Y. B. (2010). Carbon capture storage and processing as a means of enhancing renewable energy sources in Nigeria. *Renewable and Alternative Energy for Sustainable National Development*, 2, 219–225.
47. Kaisan, M. U., Naifu, T., Habib, Y. B. (2016). Towards new policies in minimizing green house gas emission in Nigeria. *Renewable and Alternative Energy for Sustainable National Development*, 2, 306–316.
48. Nafiu, T., Magaji, U. I., Zuru, A. A., Kaisan, M. U., Habib, Y. B. (2011). Production of biodiesel from wild grape seeds. *Technical Transaction Journal of Nigerian Society of Engineers*, 46, 1–10.
49. Kaisan, M. U., Pam, G. Y., Kulla, D. M. (2013). Physico-chemical properties of biodiesel from wild grape seeds oil and petro-diesel blends. *American Journal of Engineering Research*, 2, 291–297.
50. Kaisan, M. U., Pam, G. Y. (2013). Determination of engine performance parameters of a stationary single cylinder compression engine run on biodiesel from wild grape seeds/diesel blends of engine performance parameters using biodiesel from wild grape seeds. *Journal of Energy, Environment and Carbon Credit*, 3, 15–21.
51. Muhammad, S. B., Kaisan, M. U., Cyprian, O. U., Sani, F., Abdulkadir, M. (2014). Performance evaluation of a save 80 cook stoves using controlled cooking test method. *Journals of Energy Environment and Carbon Credits*, 4, 25–30.
52. Kaisan, M. U., Pam, G. Y., Kulla, D. M., Kehinde, A. J. (2015). Effects of oil extraction method on biodiesel production from wild grape seeds: A case study of soxhlet extraction method and mechanical press engine driven expeller method. *Journal of Alternate Energy and Technologies*, 6, 35–41.
53. Kela, R., Tijjani, A., Kaisan, M. U. (2015). Current status of research and development (R&D) activities on efficient cook stoves in Nigeria. *Journal of Energy Policy, Research and Development*, 1(20), 53–61.
54. Kaisan, M. U., Anafi, F. O., Nuszkowski, J., Kulla, D. M., Umaru, S. (2016). GC-MS analyses of biodiesel produced from cotton seed oil. *Nigerian Journal of Solar Energy*, 27, 56–61.
55. Kaisan, M. U., Anafi, F. O., Nuszkowski, J., Kulla, D. M., Umaru, S. (2017). Calorific value, flash point and cetane number of biodiesel from cotton, jatropha and neem oil binary and multi-blends with diesel. *Biofuels*, 8, 1–7.
56. Narayan, S., Gupta, V. (2021). Frequency characteristics of in cylinder pressure of a gasoline engine. *Journal of Applied Engineering Science*, 19(1), 92–97.
57. Narayan, S. (2015). Modelling of noise radiated from engines. *SAE Technical Papers*. DOI 10.4271/2015-01-0107.
58. Narayan, S. (2015). Effects of various parameters on piston secondary motion. *SAE Technical Papers*. DOI 10.4271/2015-01-0079.
59. Narayan, S. (2015). Analysis of noise emitted from diesel engines. *Journal of Physics Conference Series*, 662, 012018. DOI 10.1088/1742-6596/662/1/012018.